Nayak et al., http://www.jgp.org/cgi/content/full/jgp.201110752/DC1

Effect of Cs^+ on the unliganded gating equilibrium constant, E_0

Although extracellular Na^+ and K^+ did not have any effect on the unliganded gating equilibrium constant, E_0, high concentrations of extracellular Cs^+, however, did increase E_0 and the cluster open probability (Fig. S4 A and Table S5). To quantify the effect of Cs^+, we plotted the cluster open probability (P_o) versus the [Cs^+] and fitted it by the Hill equation:

$$P_o = \frac{[Cs^+]^n}{(EC_{50} + [Cs^+]^n)}.$$

At +70 mV, the effect of Cs^+ was half-maximal at ∼9.8 mM, with a Hill coefficient of 0.98 (Fig. S4 A, right). The unliganded gating equilibrium constant was approximately six times greater in 100 mM of extracellular Cs^+ compared with Na^+ or K^+. The increase in P_o at 100 mM Cs^+ was almost exclusively caused by a decrease in the channel-closing rate constant (Φ^{Cs+} = 0.03; not depicted).

Previous studies have shown that mutations of the transmitter binding site mainly influence the opening rate constant (have characteristic Φ values near 1), whereas most of those in the transmembrane domain mainly influence the closing rate constant (have Φ values closer to 0; Grosman and Auerbach, 2000; Purohit et al., 2007). Given the low Φ value and the Hill coefficient of ∼1.0, we hypothesized that the site of action of Cs^+ was in the pore rather than at the transmitter binding sites. To test this idea, we compared the unliganded gating rate constants at different voltages with and without 3 mM Cs^+ added to the pipette solution (PBS). Fig. S4 B shows that this low concentration of extracellular Cs^+ prolonged the open times (relative to the Na^+ condition) when the membrane potential was −100 mV (inward currents) but had no effect at +70 mV (outward currents). This result is consistent with the site of action of Cs^+ being within the electric field of the membrane, i.e., in the pore rather than at the transmitter binding sites.

REFERENCES

Cadugan, D.J., and A. Auerbach. 2010. Linking the acetylcholine receptor-channel agonist-binding sites with the gate. *Biophys. J.* 99:798–807. http://dx.doi.org/10.1016/j.bpj.2010.05.008

Grosman, C., and A. Auerbach. 2000. Kinetic, mechanistic, and structural aspects of unliganded gating of acetylcholine receptor channels: A single-channel study of second transmembrane segment 12′ mutants. *J. Gen. Physiol.* 115:621–635. http://dx.doi.org/10.1085/jgp.115.5.621

Hibbs, R.E., and E. Gouaux. 2011. Principles of activation and permeation in an anion-selective Cys-loop receptor. *Nature.* 474:54–60. http://dx.doi.org/10.1038/nature10139

Jha, A., P. Purohit, and A. Auerbach. 2009. Energy and structure of the M2 helix in acetylcholine receptor-channel gating. *Biophys. J.* 96:4075–4084. http://dx.doi.org/10.1016/j.bpj.2009.02.030

Jha, A., S. Gupta, S.N. Zucker, and A. Auerbach. 2012. The energetic consequences of loop 9 gating motions in acetylcholine receptor-channels. *J. Physiol.* 590:119–129.

Mitra, A., T.D. Bailey, and A.L. Auerbach. 2004. Structural dynamics of the M4 transmembrane segment during acetylcholine receptor gating. *Structure.* 12:1909–1918. http://dx.doi.org/10.1016/j.str.2004.08.004

Purohit, P., and A. Auerbach. 2009. Unliganded gating of acetylcholine receptor channels. *Proc. Natl. Acad. Sci. USA.* 106:115–120. http://dx.doi.org/10.1073/pnas.0809272106

Purohit, P., and A. Auerbach. 2010. Energetics of gating at the apo–acetylcholine receptor transmitter binding site. *J. Gen. Physiol.* 135:321–331. http://dx.doi.org/10.1085/jgp.200910384

Purohit, P., A. Mitra, and A. Auerbach. 2007. A stepwise mechanism for acetylcholine receptor channel gating. *Nature.* 446:930–933. http://dx.doi.org/10.1038/nature05721

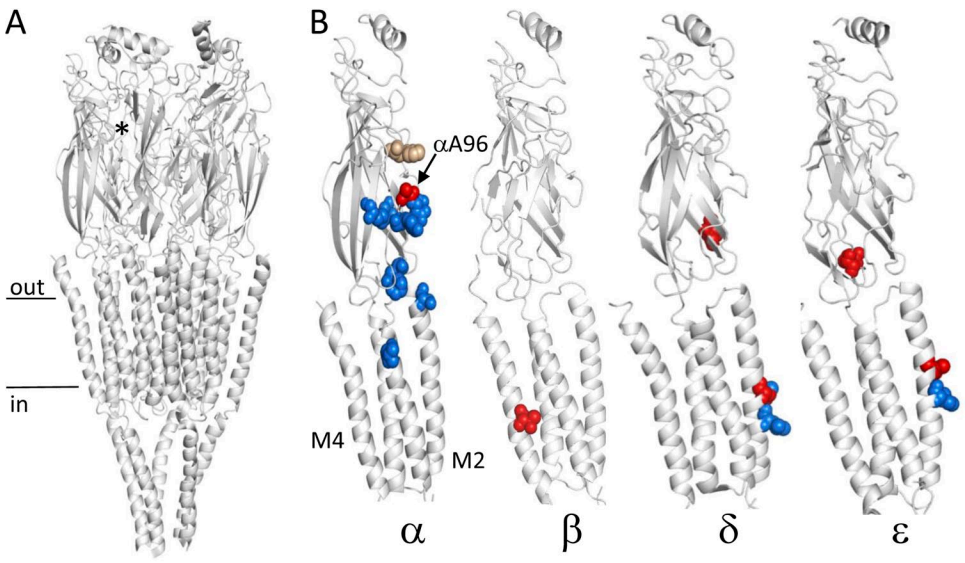

Figure S1. Locations of the mutated amino acids. (A) The *Torpedo* AChR (Protein Data Bank accession no. 2bg9). There are five subunits ($\alpha_2\beta\delta\varepsilon$ in adult type). Horizontal lines mark approximately the membrane. The extracellular domain is mostly β sheet and connecting loops and contains the two transmitter binding sites, located at the interfaces between the α and δ or ε subunits (asterisk marks the α–ε site). The transmembrane domain of each subunit has four helices. M2 lines the pore, and M4 faces the membrane. (B) Mutations by subunit. Only the extracellular and transmembrane domains are shown. Blue, the first mutation set; red, the second mutation set (see Fig. 2). The binding site residue αW149 is colored tan. The full list of mutations is given in Table S1. The location of the mutations is only approximate (Hibbs and Gouaux, 2011).

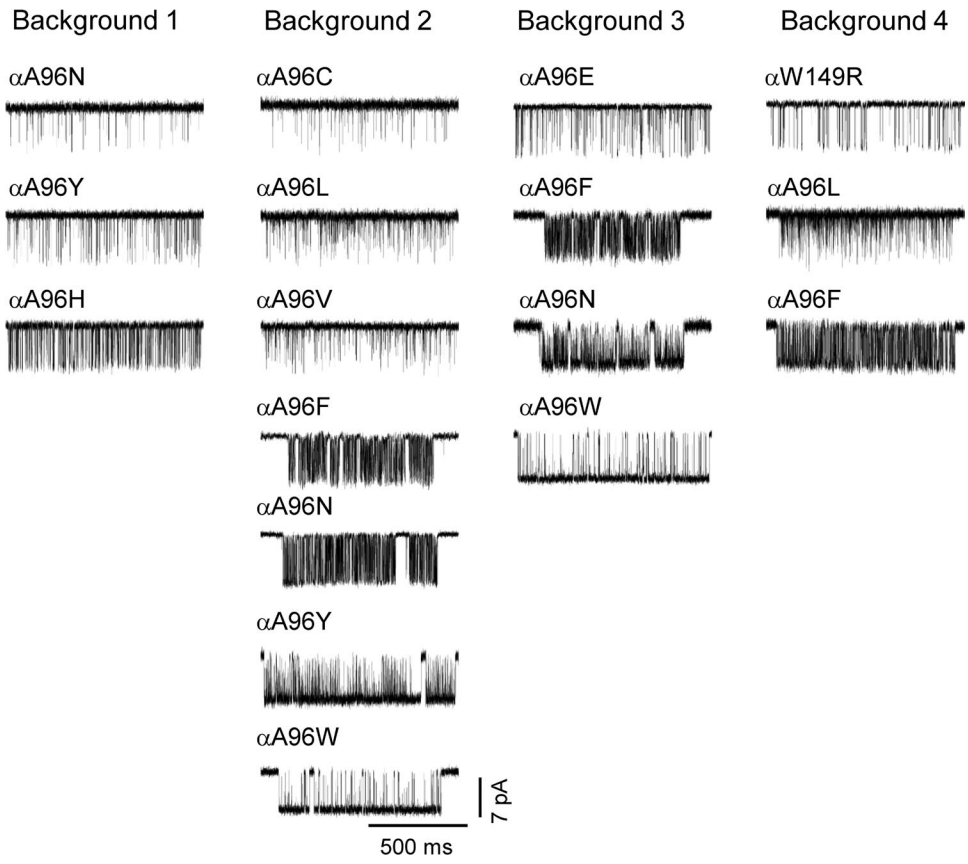

Figure S2. High resolution view of example unliganded currents from nine different side chains of A96 (C, E, F, H, L, N, V, W, and Y; set II) on four different backgrounds. Background 1, βT456I; background 2, βT456I + εE181T + εL269F; background 3, βT456I + εE181W + εL269F; background 4, βT456I + δI43Q + εE181T + εL269F. All recordings were done at −100 mV. The clusters (top to bottom) and the backgrounds (left to right) are arranged with increasing open probability, P_o. The unliganded gating equilibrium constant for each mutant combination (E_0^{obs}) was calculated as the ratio of the opening/closing rate constants from events within clusters (Table S2).

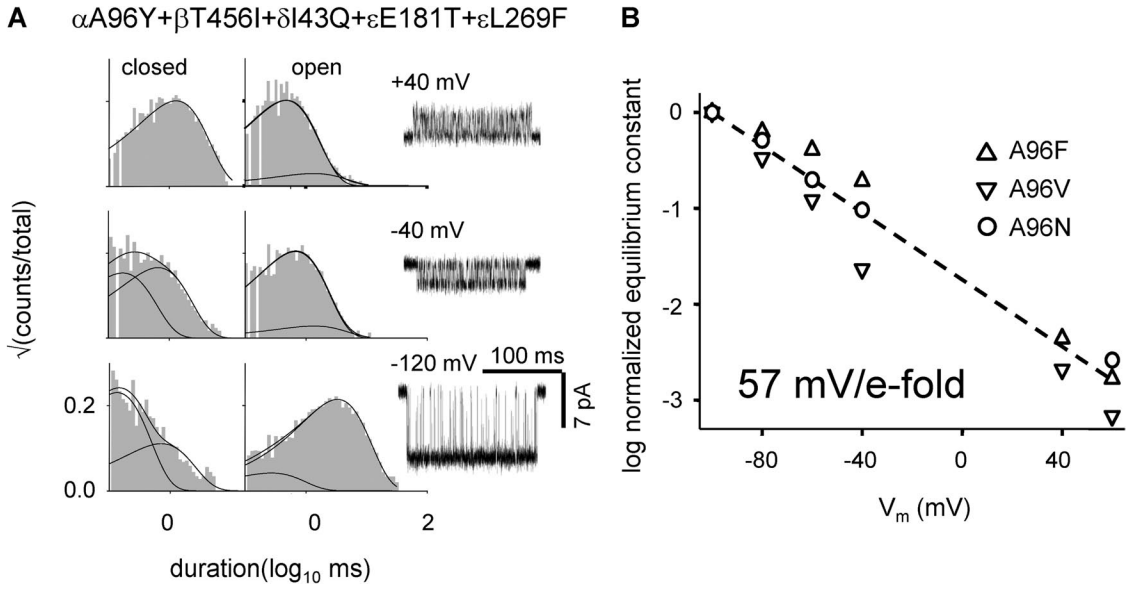

Figure S3. Voltage dependence of the unliganded gating equilibrium constant (E_0). (A) Interval duration histograms and example currents at different membrane potentials. The construct is αA96Y + βT456I + δI43Q + εE181T + εL269F. There was no ligand in the bath or the pipette. Note the decrease in closed-channel lifetime and concurrent increase in the open-channel lifetime with hyperpolarization. (B) E_0 as a function of the membrane voltage (V_m). There was an e-fold decrease in the gating equilibrium constant with a depolarization of ∼57 mV for αA96F (upward triangle), V (downward triangle), and N (open circle) (see Table S4).

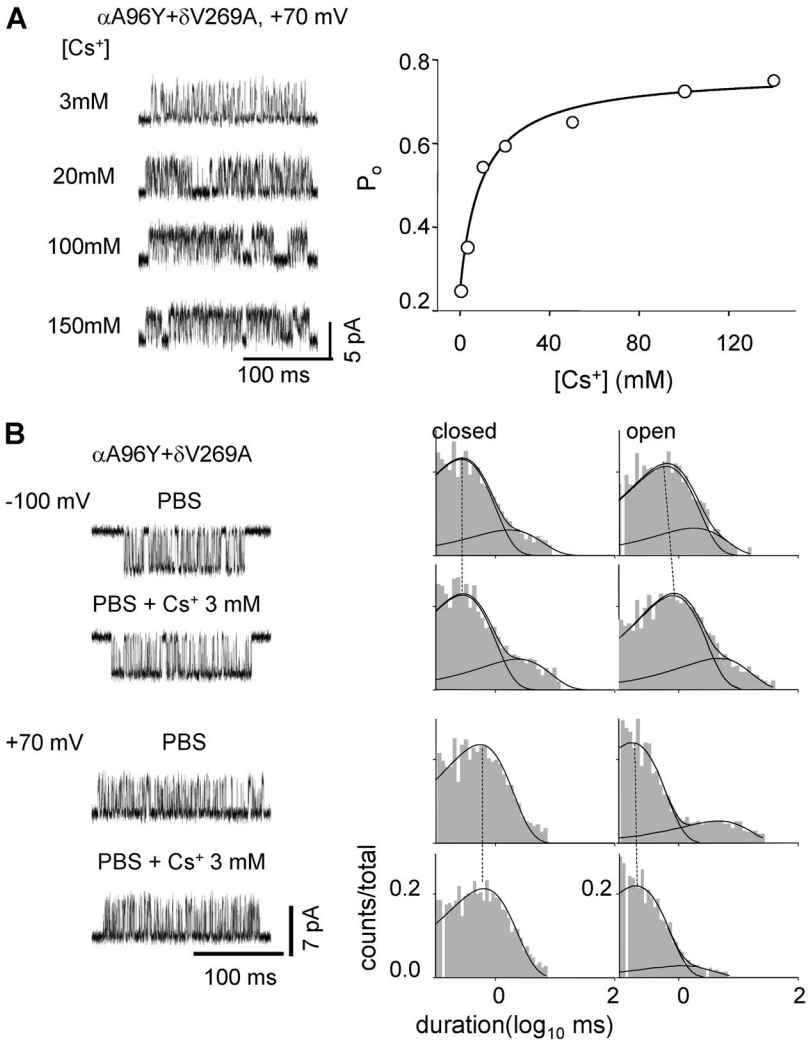

Figure S4. Extracellular Cs^+ and cluster open probability (P_o). (A) Adding Cs^+ to the pipette solution (0.1 mM $CaCl_2$) increases P_o. (Left) Example clusters of single-channel currents at +70 mV. (Right) P_o versus [Cs^+]. The half-maximal effect is at ~9.8 mM, and the Hill coefficient is 0.98 (fitted line). (B) Effect of adding 3 mM Cs^+ to the pipette solution (PBS) is voltage dependent. There is no effect of Cs^+ at +70 mV (outward currents, bottom panel), whereas at −100 mV (inward currents, top panel), 3 mM Cs^+ decreases the closing rate constant (b_0^{PBS} = 1,108 s^{-1} and $b_0^{PBS+3Cs+}$ = 787 s^{-1}).

Table S1

List of set 2 mutants and their effect on the gating equilibrium constant

Mutant	Subunit	Secondary structure	Fold increase in gating equilibrium constant	Agonist; reference
A96L	α	Loop A	49.6	Cho; Cadugan and Auerbach, 2010
A96C	α	Loop A	118	Cho; Cadugan and Auerbach, 2010
A96V	α	Loop A	197	Cho; Cadugan and Auerbach, 2010
A96E	α	Loop A	420	Cho; Cadugan and Auerbach, 2010
A96F	α	Loop A	497	Cho; Cadugan and Auerbach, 2010
A96N	α	Loop A	4,071	Cho; Cadugan and Auerbach, 2010
A96W	α	Loop A	11,800	None; Cadugan and Auerbach, 2010
A96Y	α	Loop A	18,800	Cho; Cadugan and Auerbach, 2010
A96H	α	Loop A	117,000	None; Cadugan and Auerbach, 2010
T456I	β	M4	2.1	Cho; Mitra et al., 2004
T456F	β	M4	5.0	Cho; Mitra et al., 2004
I43Q	δ	β1 strand	5	Cho; unpublished data
E181T	ε	Loop 9	2.2	Cho; Jha et al., 2012
L269F	ε	M2	179	Cho; Jha et al., 2009
V269A	δ	M2	250	Cho; Purohit and Auerbach, 2009
W149R	α	Loop B	17.1	None; Purohit and Auerbach, 2010

The fold increases in the gating equilibrium constant are with choline (Cho) except αA96H/W (none) from experimental gating equilibrium constant measurements (e.g., $[(E_2)^{mut}/(E_2)^{wt}]$). The locations of the mutants are shown in Fig. S1. E_2 fold change for αA96Y was measured by adding mutations that reduced E_0 (αV261D, 1,175-fold; αV261F, 65-fold). For the mutations used in set 1, see Purohit and Auerbach (2009).

Table S2

Effects of mutant combinations on E_0

Sl no.	Construct	Observed f_0 (s^{-1})	Observed b_0 (s^{-1})	E_2^{muts}/E_2^{wt}	Observed E_0^{mut}	n
1	αA96N βT456I	47.5 (2.9)	7,918 (830)	8.6E03	0.0063 (0.001)	4
2	αA96L βT456I ETLF	337 (57)	10,473 (595)	3.4E04	0.033 (0.006)	5
3	αA96Y βT456I	183 (52)	5,633 (641)	3.7E04	0.0324 (0.004)	5
4	αA96N αW149S	381 (15)	7,277 (1,069)	5.9E04	0.054 (0.005)	5
5	αW149R βT456I δI43Q ETLF	57(6.3)	1,136 (61)	7.31E04	0.0504 (0.006)	3
6	αA96C βT456I ETLF	293 (6.3)	4,087 (130)	9.61E4	0.072 (0.005)	2
7	αA96Y δI43Q	877 (175)	11,307 (764)	1.03E05	0.0826 (0.009)	5
8	αA96H	181 (46)	5,463 (476)	1.17E05	0.033 (0.007)	6
9	αA96V βT456I ETLF	479 (10)	6,729 (760)	1.30E05	0.074 (0.009)	5
10	αA96L βT456I δI43Q ETLF	1,445 (195)	13,723 (628)	1.78E05	0.11 (0.019)	4
11	αA96H βT456I	330 (25)	2,392 (201)	2.3E05	0.14 (0.014)	3
12	αA96E βT456I EWLF	1,060 (32)	2,674 (437)	6.3E05	0.42 (0.087)	3
13	αA96F βT456I EWLF	2,466 (238)	3,671 (185)	7.5E05	0.675 (0.068)	4
14	αA96F δI43Q ETLF	2,218 (639)	2,479 (397)	8.8E05	0.95 (0.12)	3
15	αA96F βT456I δI43Q ETLF	1,732 (108)	1,281 (77)	1.76E06	1.37 (0.14)	4
16	αA96N βT456I ETLF	2,562 (362)	1,635 (75)	2.8E06	1.56 (0.167)	4
17	αA96Y δV269A	3,849 (467)	1,108 (79)	4.7E06	3.46 (0.24)	7
18	αA96N βT456I EWLF	3,948 (185)	803 (60)	6.2E06	4.94 (0.14)	3
19	αA96Y ETLF	5,569 (422)	1,913 (75)	6.9E06	2.904 (0.1)	3
20	αA96W βT456I ETLF	4,388 (618)	368 (70)	8.5E06	12.6 (1.7)	7
21	αA96Y βT456I ETLF	9,050 (423)	911 (127)	1.34E07	10.56 (1.2)	6
22	αA96N βT456I δI43Q ETLF	6,305 (419)	525 (35)	1.52E07	13.6 (2.3)	2
23	αA96W βT456I EWLF	4,556 (450)	265 (22)	1.79E07	17.45 (2.14)	3
24	αA96W βT456I δI43Q ETLF	2,463 (406)	69 (7.8)	4.2E07	36.3 (4.6)	4
25	αA96Y βT456I δI43Q ETLF	11,400 (358)	583 (63)	6.67E07	19.9 (3.5)	5
26	αA96YαW149FβT456F	369 (56)	2,769 (472)	—	0.15	5
27	αA96HαW149MβT456F	232 (13)	3,223 (315)	—	0.07	2

ETLF = εE181T + εL269F and EWLF = εE181W + εL269F. E_2^{muts}/E_2^{wt} is the product of the fold increases in E_2 for individual mutations in the construct. f_0 and b_0 are the experimentally observed unliganded opening and closing rate constants, in s^{-1}. n is number of patches, and the numbers in parentheses are ± SEM.

Table S3

Voltage dependence of the unliganded (E_0) or diliganded (E_2) gating rate and equilibrium constant*

Construct	Ligand	V_m	Observed f_0 (s^{-1}) or f_2*(s^{-1})	Observed b_0 (s^{-1}) or b_2 (s^{-1})	Observed E_0 or E_2*	*n*
		mV				
αA96Y δV269A	None	−120	4,275 (534)	942 (107)	4.54 (0.86)	3
		−100	3,849 (208)	1,108 (84)	3.46 (0.57)	5
		−80	3,375 (255)	1,568 (72)	2.15 (0.12)	4
		−60	3,036 (98)	1,746 (153)	1.73 (0.24)	3
		−40	2,755 (196)	1,880 (121)	1.46 (0.16)	3
		+40	2,187 (112)	4,613 (327)	0.47 (0.04)	2
		+60	1,655 (183)	4,483 (70)	0.36 (0.01)	4
αA96Y βT456I δI43Q ETLF	None	−120	7.562 (697)	464 (41)	16.3 (2.3)	2
		−100	8,651 (343)	740 (28)	11.7 (0.9)	4
		−80	7,245 (912)	1,003 (78)	7.22 (1.7)	3
		−60	6,716 (635)	1,605 (56)	4.18 (0.74)	4
		−40	5,974 (294)	2,006 (173)	2.97 (0.43)	3
		+40	2,021 (367)	2,487 (307)	0.81 (0.16)	2
		+60	1,800 (223)	3,617 (488)	0.49 (0.08)	3
αA96Y δV269A	Choline	−120	3,748 (532)	230 (47)	16.3 (3.1)	2
		−100	2,845 (219)	234 (31)	12.1 (1.6)	3
		−80	2,473 (182)	275 (49)	8.9 (1.2)	3
		−60	2,075 (117)	338 (27)	6.1 (0.7)	3
		−40	1,710 (185)	506 (38)	3.0 (0.9)	3
		+40	770	813	0.96	1
		+60	840 (103)	1,177 (142)	0.71 (0.21)	2
εE181T εL269F	Choline	−120	700 (186)	175 (34)	4.0 (0.6)	2
		−100	697 (152)	198 (27)	3.5 (0.53)	2
		−80	540 (67)	330 (16)	1.63 (0.11)	3
		−60	432 (42)	372 (21)	1.16 (0.09)	3
		−40	288 (11)	490 (27)	0.59 (0.04)	3
		—	—	—	—	
		+60	160 (14)	1,349 (201)	0.11 (0.01)	2
εL269F	Choline	−100	1,560	111.64	13.97	1
		−90	1,451	106.86	13.58	1
		−80	1,083	113.73	9.52	1
		−70	1,423	114.54	12.42	1
		−60	1,214	170.68	7.11	1
		−50	1,317	172.62	7.63	1
		−40	1,115	207.47	5.37	1
		−30	862	270.93	3.18	1
		40	367	748.00	0.49	1
		50	710	1,400.18	0.51	1
		60	1,061	1,059.67	1.00	1
		70	785	1,889.02	0.42	1
		80	719	1,270.31	0.57	1
		90	698	1,118.79	0.62	1
		100	725	1,189.00	0.61	1

Table S3 (Continued)

Construct	Ligand	V_m	Observed f_0 (s^{-1}) or f_2*(s^{-1})	Observed b_0 (s^{-1}) or b_2 (s^{-1})	Observed E_0 or E_2*	*n*
εS450A	Choline	−120	180	274.73	0.66	1
		−100	161	388.44	0.41	1
		−80	180	667.88	0.27	1
		−60	157	709.61	0.22	1
		−40	85	788.32	0.11	1
		−20	85	1,205.31	0.07	1
		20	121	4,869.43	0.02	1
		40	111	2,827.34	0.04	1
		60	112	2,732.52	0.04	1
		80	115	3,142.45	0.04	1
		100	98	4,620.24	0.02	1
		120	133	3,967.00	0.03	1
DYS + δL265T	None	−100	168	91	1.85	1
		−90	110	119	0.92	1
		−80	126	103	1.22	1
		−70	113	124	0.91	1
		−60	103	114	0.90	1
		−50	99	150	0.66	1
		−40	100	171	0.58	1
		−35	100	172	0.58	1
		−30	92	152	0.61	1
		−25	93	178	0.52	1
		25	42	171	0.25	1
		30	64	269	0.24	1
		40	67	307	0.22	1
		50	77	405	0.19	1
		60	70	444	0.16	1
		70	75	482	0.16	1
		80	70	580	0.12	1
		90	72	667	0.11	1
		100	71	739	0.10	1
αDY + βδ + εL269F + εP245L	None	−100	672	1,403	0.48	1
		−80	687	1,824	0.38	1
		−60	584	2,216	0.26	1
		−40	395	2,196	0.18	1
		−25	312	2,334	0.13	1
		25	242	4,691	0.05	1
		40	197	5,418	0.04	1
		60	195	7,745	0.03	1
		80	237	9,191	0.03	1
		100	217	11,162	0.02	1

f_0 and b_0 are the unliganded opening and closing rate constants. f_2* and b_2 are the apparent diliganded opening and closing rate constants. E_0 and E_2* are the unliganded and apparent diliganded gating equilibrium constant. *n* is the number of patches, and the values in the parentheses are ± SEM.

Table S4

ΔV_m required for e-fold change in unliganded gating equilibrium constant (E_0)

Construct	ΔV_m for *e*-fold change
αA96F βT456I δI43Q ETLF	55.4 ± 3.1
αA96V βT456I δI43Q ETLF	52.6 ± 5.6
αA96N βT456I δI43Q ETLF	61.6 ± 0.8
αA96Y βT456I δI43Q ETLF	57.8 ± 2.5

ETLF = εE181T + εL269F. The unliganded gating equilibrium constant (E_0) decreased by e-fold with ∼57-mV change in membrane voltage (ΔV_m).

Table S5

Effect of monovalent cations on the unliganded gating equilibrium constant (E_0) construct: αA96Y δV269A

$[Cs^+]$	Observed f_0 (s^{-1})	Observed b_0 (s^{-1})	Observed E_0 (+70 mV)	*n*
mM				
0	1,892 (148)	5,710 (494)	0.34 (0.029)	2
3	2,407 (124)	4,412 (235)	0.54 (0.022)	4
10	2,534 (23)	2,123 (330)	1.25 (0.11)	4
20	3,020 (122)	2,064 (78)	1.46 (0.08)	3
50	3,456 (74)	1,852 (99.6)	1.89 (0.13)	2
100	3,673 (145)	1,630 (122)	2.28 (0.23)	3
150	4,074 (167)	1,382 (8.1)	2.94 (0.13)	4
H_2O	1,910 (78)	5,473 (216)	0.35 (0.026)	4
Na^+ (137)	1,637 (101)	5,688 (97)	0.29 (0.018)	4

f_0 and b_0 are the experimentally measured opening and closing rate constants, and E_0 is the unliganded gating equilibrium constant. All the recordings were done at +70 mV. The experimental f_0, b_0, and E_0 for unliganded gating with H_2O and 137 mM Na^+ in the pipette are shown for comparison. *n* is the number of patches, and the values in the parentheses are ± SEM.